Noname manuscript No.
(will be inserted by the editor)

Micropumps for Drug Delivery Systems: A New Semi-Linear Elliptic Boundary Value Problem

Mario Versaci · Nadia Mammone · Cosimo Ieracitano · Francesco Carlo Morabito

Received: date / Accepted: date

Abstract In this paper, a new differential model for electrostatic membrane micropumps for drug delivery systems is presented. In particular, a new two-dimensional nonlinear second-order differential model with singularity has been determined in steady-state conditions in which the electric field magnitude has been considered proportional to the mean curvature of the membrane. Then, a result of the existence of at least one solution for the model has been obtained although, concerning the uniqueness of the solution, it is not guaranteed. Moreover, the stability of the solutions has been studied highlighting that when a solution exists, then it is unstable. Moreover, the problem was numerically solved by means of three-stage Lobatto IIIa formula achieving the ranges of the electromechanical parameters of the material constituting the membrane with or without ghost solutions. Finally, a criterion to select the

Mario Versaci
Dipartimento di Ingegneria Civile Energia Ambiente e Materiali, "Mediterranea" University, Via Graziella Feo di Vito, I-89122 Reggio Calabria, Italy
Tel.: +39 0965 169273
E-mail: mario.versaci@unirc.it

Nadia Mammone
Dipartimento di Ingegneria Civile Energia Ambiente e Materiali, "Mediterranea" University, Via Graziella Feo di Vito, I-89122 Reggio Calabria, Italy
Tel.: +39 0965 169224

Cosimo Ieracitano
Dipartimento di Ingegneria Civile Energia Ambiente e Materiali, "Mediterranea" University, Via Graziella Feo di Vito, I-89122 Reggio Calabria, Italy
Tel.: +39 0965 169224

Francesco Carlo Morabito
Dipartimento di Ingegneria Civile Energia Ambiente e Materiali, "Mediterranea" University, Via Graziella Feo di Vito, I-89122 Reggio Calabria, Italy
Tel.: +39 0965 169224

intended use of the micropump starting from the electromechanical properties of the membrane and a criterion to choice the material constituting the membrane starting from the intended use of the micropump are presented.

Keywords Electrostatic actuators and transducers · Singularities · Difffer-ential geometry of the surfaces · Curvatures

1 Introduction to the Problem

Administering medical therapy in an efficient, targeted way is a key topic in drug delivery research. The ultimate goal is to keep the release dose at minimum while maximizing the efficacy of the drug. Delivering drugs at a specific rate would also ensure that the requirements due to the pharmacokinetic properties would be fulfilled and the efficacy of the drug will be improved [1]. Medical drugs hold the most diverse physio-chemical and pharmacokinetic properties and conventional ways of administration (oral or intravenous) are not often the most suitable ones. Such ways indeed come with several drawbacks: they may cause mild to severe side effects [2], weaken as the the drug flows through the gastrointestinal path and hence lose efficacy and require a larger dosage to ensure the drug reaches the desired the target site at a proper therapeutic drug concentration [3–5]. Targeted delivery is of paramount importance when administering pharmaceuticals that have short half-lives in vivo or that are very toxic [6]. Furthermore, the possibility to administrate therapy locally would have a great impact on the treatment of the parts of the body that can be hardly reached by pharmaceuticals because of physical barriers like, for example, the brain and the posterior part of the eyes, that can be hardly reached through conventional intravenous administration. Transdermal systems cannot ensure a precise and efficient drug delivery, this is the reason why the attention of the scientific community is focused on micro-systems, either implantable or non-implantable [7]. Micro-technology or Micro-electromechanical Systems (MEMS) is a promising technology in the field of novel drug delivery systems' development. Micro-technology indeed allows to deliver a wide variety of drugs with high therapeutic efficacy. They allow for miniaturization [8,9], integration [10,11] and electromechanical control [11]. MEMS devices include micro-particles, micro-reservoirs, bio-capsules, micro-needles, and implantable micropumps [6]. MEMS micropump technology allows to release drugs at a specific rate, according to the specific drug's pharmacokinetic properties, MEMS also allows to control infusion volumes and also ensure a continuous drugs' supply through a reservoir [12]. Implantable subcutaneous drug delivery, although invasive, has several advantages. It allows for a long-term drug administration (for example in case of insulin or of cancer therapy) with no need of repeated needle injection, in this way making drug administration independent from the subject's daily activity, improving the quality of the subject's life and reducing the need of hospitalization. A micropump is a mechanical or non-mechanical pump whose dimension ranges in a

micrometer scale, there are different kind of mechanical micropumps: electrostatic, thermo-pneumatic, piezoelectric, shape memory alloy, ionic conductive polymer film, bimetallic [3].
This paper focuses on the first category: micropumps based on electrostatic actuation mechanisms. Electrostatic micropumps consist of an inlet and an outlet valves, two counter electrodes, an actuation chamber, a pump chamber and a membrane (Figure 1). The membrane gets attracted or repelled by an electrostatic force $\mathbf{F}$, generated by the voltage V between the two counter electrodes producing the pumping action [13]. Periodical membrane inflection/deflection can be produced by switching periodically V [14], [15],[3]. The main drawbacks of electrostatic micropumps are that high voltages are required, membrane deflection is limited and only of non-conductive fluids can be pumped [3]. In [16], a bidirectional electrostatic micropump for miniaturized chemical analysis systems with a silicon pump that incorporated two passive check valves has been developed. In [17] an electrostatic micropump that required a very small flow rate, meant for drug delivery applications was studied. In [18], a methodology was proposed to predict the state of an electrostatic micropump at equilibrium. The model was based on the minimization of the overall energy which included: the energy of the fluid, the capacitive energy and the diaphragm's strain energy. In this paper, a novel differential model for electrostatic membrane micropumps for drug delivery systems is introduced. Given a voltage V, applied between the two counterelectrodes, an electrostatic field $\mathbf{E}$ is generated which produces an electrostatic pressure p_{el} which induces a mechanical pressure p. In this way, the membrane is deflected, the average deflection is proportional to $|\mathbf{E}|$. A second order nonlinear differential model with singularity is derived, which does not allow to find a closed-form solution (i.e. membrane's profile). To overcome this issue, upper- and lower-bound solutions are found, through an analytical approach based on finding specific upper- and lower-solutions of the membrane's profile. In this way, an algebraic condition that ensures the existence of at least one solution is derived. Even though the solution's existence is ensured, the uniqueness is not guaranteed. However, this paper proves that the stability of the membrane is not guaranteed when the solution exists. Moreover, the electromechanical properties of the material determine the intended use of the micropump. In this regard, in this work, we present a simple criterion that, starting from these electromechanical properties, we select the intended use of the micropump. Moreover, some numerical tests, based on three-stage Lobatto IIIa formula [19], [20], have been performed to achieve ranges of the electromechanical parameters with or without ghost solution (i.e., solutions obtained numerically that do not satisfy the analytical condition of existence and uniqueness for the solution) and the different areas where ghost solutions take places. Finally, a further criterion proposed in this work helps us to choose the material constituting the membrane once the intended use of the micropump has been chosen and vice-versa.
The paper is organized as follows. Starting from Section 2 in which an overview of the previous works is reported, Section 3 describes the circular membrane micropump device. Two points are taken into account: the first one, is related

Symbols	Meaning	Symbols	Meaning
$\mathbf{F}$	electrostatic force	V	voltage
$\mathbf{E}$	electrostatic field	p	mechanical pressure
L	length of the $1D$ device	d	distance between the plates
v	profile of the membrane	T	mechanical tension of the membrane
ϵ	permittivity of the free space	C	curvature of the membrane
$\theta\lambda^2$	characteristics parameters of the membrane	R	radius of the disks
r	radial coordinate	d^*	critical security distance
p_{el}	electrostatic pressure	C_{el}	capacitance
$\overline{q}$	thickness of the plate	D	flexural stiffness
v_0	displacement at the center of the plate	μ	function of proportionality
MC	mean curvature	v_1, v_2	lower and upper solutions

Table 1: List of the main symbols

to the actuator (Subsection 3.1) and the second one concerns the transducer (Subsection 3.2). Then, after some considerations about both mechanical and electrostatic pressures (Subsection 3.3) and how the transducer can help the performance of the actuator (Subsection 3.4), the model is revised in terms of mean curvature (Sections 4). Then, after some well-known preliminary results, Section 5 details the determined condition ensuring the existence of at least one solution, and Section 6 explains why the problem does not admit uniqueness of the solution. Once the instability of the solution has been verified (Section 7), the numerical tests perfomed are detailed in Section 8. Then, the above mentioned criteria about the intended use of the micropump and the characteristic electromechanical of the material constituting the membrane are proposed (Section 9). Finally some concluding remarks as well as ideas for future works complete the work. To improve the readability of the paper, a list of the main symbols is shown in Table 1.

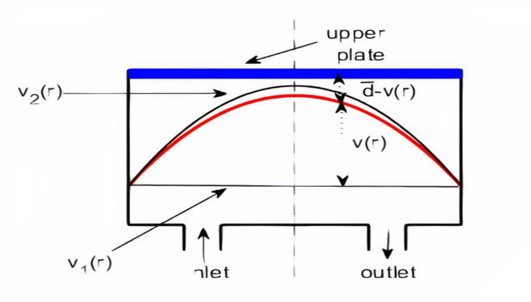

Fig. 1: The basic electrostatic micropump. $v(r)$ vs r: visualization of $v(r)$, $1 - v(r)$, d^* and upper and lower solutions $v_1(r)$ and $v_2(r)$.

2 An Overview of the Previous Works

In [21] a $1D$ model of a steady-state micro-electro-mechanical system has been studied. It consisted of two parallel metallic plates (with length is L), distant from each other by a quantity d: the lower one is fixed and the upper one is deformable but clumped at the boundary of a region $\Omega \in \mathbb{R}^N$. The device is also subjected to a voltage V. Once V is applied, the deformable plate deforms. Let us indicate by $v(x)$, $x \in \Omega$, the profile of the deformed plate. As known, the analytical model is the following:

$$\begin{cases} \Delta^2 v(x) = \frac{m_1(x)\beta_1}{(1-v(x))^2} = \frac{\beta^2(x)}{(1-v(x))^2} \\ 0 \leq v(x) < 1 \ \text{ in } \Omega, \\ v = \Delta v - \hat{d} v_\nu, \ \text{ on } \partial\Omega, \ \ \hat{d} \geq 0. \end{cases} \tag{1}$$

In (1), β_1 is computable as [22] $\beta_1 = \frac{\epsilon_0 V^2 L^2}{2Td^3}$ in which T and ϵ_0 represent the mechanical tension of the plate and the permittivity of the free space, respectively; $m_1(x)$ represents a bounded function depending on the dielectric properties of the material constituting the lower plate. Moreover, $\beta(x)$ depends on both V and the dielectric properties of the material constituting the lower plate. The aforementioned analitical model (1) has been studied in detail in [23]. Specifically, the existence of at least one solution has been studied by means of Steklov boundary condition achieving both Dirichlet and Navier boundary conditions. It is worth nothing that v_ν represents the outer normal derivative of u on $\partial\Omega$ if $\hat{d} = 0$ one achieves the Navier boundary conditions and if $\hat{d} = \infty$ one obtains the Dirichlet boundary conditions. From (1), in [21], [24], [25], [26], [27], [28], a new elliptical semi-linear model for a $1D$ micro-electro-mechanical device has been studied. Specifically, it has been formulated as follows:

$$\begin{cases} v_{xx}(x) = -\frac{(1+(v_x(x))^2)^3}{\theta\lambda^2}(1-v(x))^2, \quad \text{in } \Omega = [-1, 1], \\ 0 \leq v(x) < 1, \quad v = 0 \quad \text{on } \Omega, \end{cases} \tag{2}$$

with $v_x = \frac{\partial v}{\partial x}$, $v_{xx} = \frac{\partial^2 v}{\partial x^2}$. Furthermore, it is to be noted that the deformable plate is replaced by a membrane and $|\mathbf{E}|$ is formulated proportional to the curvature of the membrane, C. In [21], results of existence for the solution to (2) have been obtained and the uniqueness condition does not depend on the electromechanical properties of the material constituting the membrane. Then, in [26], [28], [29] a new condition of uniqueness for the solution to (2) depending on those properties has been determined. Numerically, (2) has been solved by exploiting the shooting procedure (see [24], [28]); in particular, pointing out the values of $\theta\lambda^2$ and ensuring the convergence of the numerical method (without ghost solutions). In [26], [28], finally, Keller-Box and shooting approaches have been compared obtaining optimal values of $\theta\lambda^2$ (without ghost solutions).This work focuses on a $2D$ circular membrane micropump for drug delivery system [3]. We observe an axial symmetry of the membrane; the z axis is the rotation axis and v is the profile of the membrane considered as a surface generated by rotating a curve C around z on the vertical plane rz in the first quadrant, with $0 \leq r \leq R$. On this basis, one can conclude that v only depends on the radial coordinate r considering the problem as a $1D$ problem (with x replaced by r). Then, it can be noted that the only radial part of the Laplace operator can be taken into account. Hence, (1) becomes:

$$\begin{cases} v_{rr}(r) + \frac{v_r(r)}{r} = -\frac{\lambda^2(r)}{(1-v(r))^2}, \\ v(R) = 0, \quad v_r(0) = 0, \end{cases} \tag{3}$$

where $\lambda^2(r) = \beta_1(r)m_1(r)$, $\frac{1}{r}$ is a singularity and $\frac{\lambda^2(r)}{(1-v(r))^2}$ represents $|\mathbf{E}|^2$ (see [21]). Then, considering $|\mathbf{E}|$ proportional to the mean curvature MC of the membrane, model (3) can be written as follows:

$$\begin{cases} v_{rr}(r) = -\frac{v_r(r)}{r} - \frac{(1-v(r)-d^*)^2}{\theta\lambda^2}, \\ v(R) = 0, \quad v_r(0) = 0, \quad 0 < v(r) < d, \end{cases} \tag{4}$$

in which d^* represents the critical security distance ensuring that the membrane does not touch the counter-electrode when it moves. In the following of the work, we prove a result of existence of at least one solution to (4) althougth its uniqueness is not ensured.

3 Circular Membrane Micropumps

3.1 The Actuator Point of View

An electrostatic micropump is a micro device constituted by a circular membrane with radius R which moves between two parallel disks with the same radius with mutual distance d. The membrane, deforming toward the upper disk (counter-electrode) when V is applied, is clamped on the edge of the lower disk considered at $V = 0$ (Figure 1). The membrane moves towards the counter-electrode changing in volume the chamber below the membrane itself: then, the drug fluid is drawn from the inlet check valve (Figure 1). When V is removed, the membrane returns to its un-deflected position pushing out the fluid through the outlet check valve (Figure 1). Repeating these operations, the device results in a pumping action. It is worth nothing that the design of an electrostatic membrane micropump is limited to the pull-in instability. In particular, the volume under the membrane is small due to the limited range of stable displacements of the membrane [22]. However, it is imperative that the membrane smashes into the counter-electrode (pump in pull-in mode) [22]. As known, V generates inside the device an electrostatic field $\mathbf{E}$ and also an electrostatic pressure, p_{el}, deflecting the membrane [27]. It is to be noted that, during the movement of the membrane, the direction of $\mathbf{E}$ is locally normal to the tangent straight line of the membrane so that $|\mathbf{E}|$ depends on the local distance between the membrane itself and the cou nter-electrode [24]. Then, the capacitance C_{el} of the device changes because the distance between the membrane and the counter-electrode locally also changes. Obviously, p_{el} increases with $|\mathbf{E}|$, so, the mechanical pressure p increases deforming the membrane. Consequently, C will be higher. It follows that $|\mathbf{E}|$ can be locally considered to be proportional to C.

3.2 The Transducer Point of View

When a mechanical pressure p is applied to a two-plates micro device, the deformable plate moves and its deflection v satisfies the well-known partial differential equation [22] depending on ρ (density of the material constituting the plate), $\overline{q}$ and D (thickness and the flexural stiffness of the plate, respectively). In steady-state case, its solution is [22]

$$v(r) = \frac{R^4(1-(\frac{r}{R})^2)^2}{64D}p, \tag{5}$$

with $0 \leq r \leq R$, [30] from which, if $r = 0$, the displacement at the center of the plate is $v_0 = \frac{R^4}{64D}p$. Finally, $v(R) = \left(1 - \left(\frac{r}{R}\right)^2\right)^2 v_0$. On the contrary of the actuator behavior, the device behaves as a transducer: indeed, p generates $v(r)$ varying the electrostatic capacitance C_{el} [22].

3.3 p & a Circular Membrane Micropump Transducer

Considering circular membrane devices, D values are lower than when a circular plate micropump is taken into account as lower values of D mean membrane more flexible. It follows that v_0 increases, so that the membrane is next to the counter-electrode.

Remark 1 It is worth nothing that in the case of circular membrane devices v_0 increases remarkably when an external V is applied. Then, the distance between the membrane and the counter-electrode is locally equal to $1 - v(r)$.

Applying p to the membrane, it follows that

$$v_0 = \frac{0.25pR^2}{T} \tag{6}$$

so that $v(r)$ can be expressed as [22]:

$$v(r) = v_0\Big(1 - \Big(\frac{r}{R}\Big)^2\Big). \tag{7}$$

Moreover, f_{el}, taking into account Remark 1, can be expressed as [22,30] $\frac{0.5\epsilon_0\beta R^2V^2}{(1-v(r))^2}$, so that p_{el} assumes the following form:

$$p_{el} \cong \frac{f_{el}}{\beta R^2} = 0.5\frac{\epsilon_0 V^2}{(1-v(r))^2}. \tag{8}$$

It is worth nothing that when both f_{el} and p_{el} are computed, the membrane surface can be considered equal to βR^2 even when the membrane moves towards the counter-electrode. This is correct because $d \ll R$ so that the variation of the surface, when the membrane moves, is negligible.

3.4 How the Transducer "Helps" us to Understand the Performance of The Actuator

As known, when V is applied to an actuator, $\mathbf{E}$ is produced inside the device so that a p_{el} is generated deforming the membrane. It follows that a link between p and p_{el} is verified. From (6), we can say that v_0 linearly depends on p so that one can write $v_0 = 0.25\frac{pR^2}{T} = \alpha p$, where $\alpha = 0.25\frac{R^2}{T}$ (constant value). In addition, if other causes do not occur, p exclusively depends on p_{el}, i.e. $p = p(p_{el})$, so that it is possible to write the following chain of equalities:

$$v_0 = \alpha p = \alpha\beta p_{el} = k p_{el}, \tag{9}$$

with both β and k constant. Then, taking into account (8) v_0 becomes:

$$v_0 = 0.5k\frac{\epsilon_0 V^2}{(1-v(r))^2}. \tag{10}$$

In (10), $1 - v(r)$ is the distance between $v(r)$ and the counter-electrode. Since the profile of the membrane does not touch the counter-electrode (the membrane is at least d^* away), one can write $v(r) \leq d - d^*$ so that $\frac{1}{(1-v(r))^2} \leq \frac{1}{d^{*2}}$. The details can be observed in Figure **??** where a recovering of the membrane is displayed in red color. Then, locally, the distance of the membrane from the rest position and from the counter-electrode is valuable as $v(r)$ and $1 - v(r)$, respectively. Then, Eq. (7) easily becomes:

$$v(r) \leq \overline{v}(r) = \frac{0.5k}{d^{*2}}\Big(1 - \Big(\frac{r}{R}\Big)^2\Big)\epsilon_0 V^2. \tag{11}$$

It is worth nothing that the link between p and p_{el} highlights a duality in the actuator-transducer model so that the transducer help us to understand how the actuator works and vice-versa.

4 The Proposed Model: |E| Proportional to the Curvature of the Membrane

As already mentioned above, $\frac{\lambda^2}{(1-v(r))^2}$ in model (3) is proportional to $|\mathbf{E}|^2$. Hence, model (3) can be simplified to:

$$\begin{cases} v_{rr}(r) + \frac{v_r(r)}{r} = -\theta|\mathbf{E}|^2; \\ \theta \in \mathbb{R}^+, \quad v(1) = 0, \quad v_r(0) = 0. \end{cases} \tag{12}$$

We highlights that θ is a continuous function depending on r such that, if $C(r, v(r))$ is the curvature of the deformed membrane, then $|\mathbf{E}(r)|$ is considered proportional to $C(r, v(r))$ by means of a proportionality function, $\mu(r, v(r))$. It is worth nothing that $\mu(r, v(r))$ depends on both r and $u(r)$. This is due to the fact that moving along the abscissa axis, $|\mathbf{E}|$ varies. Furthermore, different membrane profiles (i.e. different $v(r)$) force different locations of $\mathbf{E}$. Then, it follows that $|\mathbf{E}(r)| = \mu(r, v(r))C(r, v(r))$. Therefore, if $\mu(r, v(r)) = \frac{\lambda}{(1-v(r)-d^*)}$, model (12) can be expressed in the following non linear form with singularity $1/r$:

$$\begin{cases} v_{rr}(r) + \frac{v_r(r)}{r} = -\theta\mu^2(r, v(r))C^2(r, v(r)) = -\frac{\theta\lambda^2 C^2(r,v(r))}{(1-v(r)-d^*)^2}, \\ \theta \in \mathbb{R}^+, \quad v(1) = 0, \quad v_r(0) = 0. \end{cases} \tag{13}$$

Obviously we need to explicitly define the curvature C. Since the problem is $2D$, we need to formulate C relative to surfaces in space. Then, formulating the curvature in terms of mean curvature MC can be a viable solution for our goals [31]. Exploiting a well-known technique of differential geometry [31], it is easy to obtain the following formulation for the mean curvature MC (for detail, see Appendix A), $MC(r) = -\frac{1}{2}\left(\frac{v_r(r)}{r} + v_{rr}(r)\right)$. Thus, the proposed model (13) can be written as follows:

$$\begin{cases} v_{rr}(r) + \frac{v_r(r)}{r} = -\frac{\left(\frac{v_r(r)}{r}+v_{rr}(r)\right)^2 \theta\lambda^2}{4(1-v(R)-d^*)^2} \\ v(1) = 0, \quad v_r(0) = 0, \quad 0 \leq v(r) < d. \end{cases} \tag{14}$$

Model (4) is a particular version of a general problem formulated on $\Omega = [m, n]$ with a singularity $1/r$ located at m. Therefore, (4) is a special case of the following general model:

$$\begin{cases} v_{rr}(r) = -\overline{P}(r, v(r), v_r(r)), \\ u(n) = S, \quad u_r(m) = t, \quad S, t \in \mathbb{R}. \end{cases} \tag{15}$$

In fact, it is sufficient to set $\overline{P}(r, v(r), v_r(r)) = \frac{v(r)}{r} + \frac{(1-v(r)-d^*)^2}{\theta\lambda^2}$, with $S = 0$, and $t = 0$, to achieve (4).

5 On the Existence of at Least One Solution

Now, we need to exploit the following results well-known in literature [22].

Result 1
On (15) we define $v_1(r)$ and $v_2(r)$ two twice continuously differentiable functions such that [32] $\forall r \in (m, n)$, $v_1(r) < v_2(r)$ and, moreover,

$$v_{1rr}(r) + P(r, v_1(r), v_{1r}(r)) > 0 \tag{16}$$

$$v_{2_{rr}}(r) + P(r, v_2(r), v_{2_r}(r)) < 0. \tag{17}$$

In addition, let us consider the continuous function $P(r, y(r), y_r(r))$, defined in $\mathcal{W} \times (-\infty, +\infty)$ with

$$\mathcal{W} = \{(r, v) \ : \ m < r < n \quad \text{and} \quad v_1(r) \leq v(R) \leq v_2(r)\},$$

satisfying the generalized Lipschitz's condition:

$$\begin{aligned} M_1(r)(v(r) - u(r)) + N_2(r)(v_r(r) - u_r(r)(r)) \leq \\ \leq P(r, v(r), v_r(r)) - P(r, u(r), u_r(r)) \leq \\ \leq M_2(r)(v(t) - u(r)) + N_1(r)(v_r(r) - u_r(r)), \end{aligned} \tag{18}$$

where $M_1(r)$, $M_2(r)$, $N_1(r)$ and $N_2(r)$ are continuous function defined on $(m, n]$. Moreover, if $v_{1_r}(m) \geq v_{2_r}(m)$, with $v_1(n) = v_2(n) = S$, then (15) has at least one solution (say, $v(r)$) in order that $v_1(r) \leq v(r) \leq v_2(r)$, $\forall r \in [m, n]$ [32].

Result 2
Supposing that all the hypothesis of Result 1 are satisfied, we suppose that both $v_1(r)$ and $v_2(r)$ satisfy the given boundary conditions. Then, if the following

$$v_{rr}(r) + M_2(r)v(r) + N_1(r)v_r(r) = 0$$

has nontrivial solution satisfying zero boundary conditions on any sub-interval of $[m, n]$, then the problem admits only one solution, $v(r)$, such that $v_1(r) \leq v(r) \leq v_2(r)$[32].
$Nowwearereadytopresentaresultofatleastonesolutionfortheproblemunderstudy.$

Proposition 1 *Let us consider the problem* (4) *and Results 1 and 2 above detailed. Let also* $v_1(r)$ *and* $v_2(r)$*, with* $v_1(r) < v_2(r)$*, be two twice continuously differentiable functions, defined on the range* $[0, R]$ *such that* $\forall r \in (0, R)$*:*

$$v_{1_{rr}}(r) + \frac{v_{1_r}(r)}{r} + \frac{(1 - v_1(r) - d^*)^2}{\theta\lambda^2} > 0 \tag{19}$$

$$v_{2_{rr}}(r) + \frac{v_{2_r}(r)}{r} + \frac{(1 - v_2(r) - d^*)^2}{\theta\lambda^2} < 0 \tag{20}$$

Moreover, let, for $r \neq 0$, $\frac{v_r(r)}{r} + \frac{(1 - v(r) - d^*)^2}{\theta\lambda^2}$ *be a continuous function satisfying the generalized Lipschitz's condition in*

$$\{(r, v) \ : \ 0 < r < R \quad \textit{and} \quad u_1(r) \leq v(R) \leq u_2(r)\} \times (-\infty, +\infty).$$

If $v_{1_r}(0) \geq v_{2_r}(0)$, $v_1(R) = v_2(R) = 0$, *and*

$$\theta\lambda^2 > \frac{2R^2 d^{*2}}{V^2 \epsilon_0 k}, \tag{21}$$

there exists at least one solution for the problem (4)*. Then,* (21) *ensures the existence of at least a solution for the problem* (4)*.*

Proof See Appendix B

We note that on the plane $d^* - \theta\lambda^2$ the parabolic line changes its position according to the values assumed by the single parameters present in the algebraic inequality which guarantees the existence of at least one solution for the model under study. Particularly, by fixing d^*, V and R, the greater k will be the smaller $\theta\lambda^2$ will be. Furthermore, since V is fixed, p_{el} will also be fixed (see (8)). Then, by means of (9), increasing k, v_0 will increase so that the membrane approaches the counter-electrode (direct problem). If, on the other hand, we fix the position of the membrane, v_0 is fixed so that, once that k is also fixed, it follows that p_{el} will be computed as v_0/k (see, (9)). Then, V will be computed by (10) (inverse problem). From the above proved algebraic condition, setting $d^* = 10^{-3}$, $R = 10^{-2}$, $\epsilon_0 \approx 10^{-12}$, we can write $\theta\lambda^2 > 0.5V^{-2}d^*R^2(k\epsilon_0^{-1}) \approx 0.5 \cdot 10^4(kV)^{-2}$. If, in addition, we introduce the equivalence between p and p_{el}, i.e. $k = 1$, we achieve $\theta\lambda^2 > 0.5 \cdot 10^4 V^{-2}$, ensuring that in (14) the quantity $v_r r(r)$ is much less than zero ensuring a significant deformation to the membrane when V (less than 1 Volt) is applied.

6 On the Uniqueness of the Solution

The following result proves that the uniqueness of the solution is not ensured.

Proposition 2 *We take it for granted that all hypotheses of the Theorem 1 are satisfied. Moreover, we suppose that both $v_1(r)$ and $v_2(r)$ satisfy the given boundary conditions. Then, we prove that the uniqueness of the solution for the problem under study* (4) *$v(r)$, with $v_1(r) \le v(r) \le v_2(r)$, is not ensured.*

Proof See Appendix C.

7 On the Stability of the Solution

Let us introduce the following Lemma [22].

Lemma 1 *Problem* (4) *admits stable equilibrium position only if its eigenvalues are not with positive real part.*

Proof See [22].

Let us consider the problem under study (4), in which we set

$$\hat{f}(v(r)) = -4\frac{(1 - v(r) - d^*)^2}{\theta\lambda^2}. \tag{22}$$

In addition, let $v^*(r)$ the root of $\hat{f}(v(r))$, that is:

$$v^*(r) = 1 - d^*. \tag{23}$$

Then, from (22) we can write $\hat{f}_r(v(r)) = \frac{8(1-v(r)-d^*)}{\theta\lambda^2}$. In addition, taking into account (23), we obtain:

$$\hat{f}(v^*(r)) = \frac{8(1 - v^*(r) - d^*)}{\theta\lambda^2} = 0. \tag{24}$$

We look for solutions whose structure is $v(r) = v^*(r) + \xi e^{-\mu r}$ with $\xi \ll 1$, μ eigenvalue, from which it follows that:

$$v_r(r) = -\mu\xi e^{-\mu r}; \quad v_{rr}(r) = \mu^2 \xi e^{-\lambda_1 r}. \tag{25}$$

Substituting both (25) in equation (4), we obtain

$$r^{-1}(-\lambda_1 \xi e^{-\lambda_1 r}) + \lambda_1^2 \xi e^{-\lambda_1 r} = f(v^*(r) + \xi e^{-\lambda_1 r}), \tag{26}$$

from which, developing $f(v^*(r) + \xi e^{-\lambda_1 r})$ in Taylor's series and taking into account that $f(v^*(r)) = 0$, we can write

$$\lambda_1^2 - \frac{\lambda_1}{r} - f'(v^*(r)) = 0 \tag{27}$$

from which we achieve

$$\lambda_1 = \frac{1}{2}\left(\frac{1}{r} \pm \sqrt{\frac{1}{r^2} + 4f'(u^*(r))}\right) \tag{28}$$

and taking into account condition (24), we obtain:

$$\frac{1}{2r} + \frac{1}{2r} = \frac{1}{r} > 0 \tag{29}$$

If (29) holds, then, it proves that the Real$\{\lambda_1\} > 0$ so that, by means Lemma 1 highlighting that the solution $v(r)$ is unstable.

8 Numerical Tests: Interesting Ranges of $\theta\lambda^2$ and Ghost Solutions Areas

Instability phenomena of the membrane arise if V grows too much, so that it is important to know the range of V generating instability. Thus, being V linked to $\theta\lambda^2$ (see (36)), the behavior of the membrane when $\theta\lambda^2$ increases gives us, if both d^* and k are fixed, the range of V producing instability of the membrane (with or without ghost solutions). We observe that by the ranges of possible values for $\theta\lambda^2$ ([1]), it is possible to know the operation parameters in convergence area respecting (36) and the engineering areas of applicability of the device. Therefore, we consider p_{el} and p equivalent each other because when V is applied $|\mathbf{E}|$ and p_{el} are generated inside the device. Here, all the simulations have been achieved by bvp4c MatLab® solver with default relative

[1] Depending on both the electromechanical properties of the material constituting the membrane and V

and absolute error tolerances achieving 100 grid points ([2]) lied to the proposed model (14) reformulated as a system of first order differential equations as follows (setting $u_1(r) = u(r)$ and $u_2(r) = u_r(r)$):

$$\begin{cases} \frac{du_1(r)}{dr} = u_2(r); \\ \frac{du_2(r)}{dr} = -\frac{u_2(r)}{r} - \frac{(1-u_1(r)-d^*)^2}{\theta\lambda^2} \\ u_1(R) = 0; \qquad u_2(0) = 0. \end{cases} \tag{30}$$

This solver has been exploited because its code implements the three-stage Lobatto IIIa formula that represents a collocation formula exploiting a polynomial providing a C^1 continuous solution (fourth-order accurate). In this work, three cases occurred.

In the first case, if $\theta\lambda^2 \in (10^{-6}, +\infty)$ no instabilities arose applying the the numerical procedure: therefore, if $\theta\lambda^2$ increased from 10^{-6}, $u_{rr}(r)$ increased from negative values towards zero. Then, the concavity of the deformed membrane decreased avoiding instabilities close to the edges. This occurrence is confirmed by (36). Figures 2 depict a typical example of recovering of the membrane when $\theta\lambda^2 = 0.5$, with an initial guesses $u_1 \leq 2.446$ and $u_2 = 0$. Here, being V small, the membrane moves towards the upper plate just a little. There, instabilities do not appear. If the initial guess of u_1 increases (with $u_2 = 0$), the behavior of the procedure is different as shown in Figures 3, 4 and 5 in which examples of recovering of the membrane are depicted when $\theta\lambda^2 = 0.5$ and with initial guess for u_1 belonging to $[2.447, 2.453]$, $[2.454, 9.474]$, $[9.63, 12.7]$ and $[15.1, 19.978]$, $[9.475, 9.62]$, $[12.71, 15]$ and $[19.979, +\infty)$, respectively (initial guess for u_2 is zero). Moreover, if the initial guess for u_1 and $u_2 = 0$ increase, the recovering of the membrane is symmetrical but erratic (see Figure 3) until the profile becomes a bell-shape (Figure 4). This erratic behavior also arise if the initial guess increasing (see Figure 5). However, even if Figures 3, 4 and 5 depict recovering of the membrane numerically correct, being $u_1 > d$, they are not realistic.

In the second case, if $\theta\lambda^2 \in (0, 10^{-7})$, the procedure does not work. In other words, $\frac{(1-u(r)-d^*)^2}{\theta\lambda^2}$ increases too much because, as $\theta\lambda^2 \to 0$, $\frac{(1-u(r)-d^*)^2}{\theta\lambda^2} \to \infty$ (the Jacobian matrix is singular).

In the last case, if $\theta\lambda^2 \in [10^{-7}, 10^{-6}]$ strong instabilities next to the edes of the membrane arise, even if the numerical method does not stop. Figures 6 (obtained setting $u_1 = 0.1$ and $\theta\lambda^2 = 5 \cdot 10^{-7}$) and 7 (achieved when $u_1 = 1.2$ and $\theta\lambda^2 = 10^{-6}$) show two typical recovering of the membrane when $\theta\lambda^2 \in [10^{-7}, 10^{-6}]$ putting in evidence strong instabilities.

Moreover, from (21), being $R = 1$, $d^* = 10^{-9}$, $k = 1$ and $\epsilon_0 \approx 10^{-12}$, we easily achieve

$$\theta\lambda^2 > \frac{R^2 {d^*}^2}{2V^2\epsilon_0 k} \approx \frac{(10^{-6})^2(10^{-9})^2}{V^2 10^{-12} k} = \frac{10^{-18}}{V^2 k} \tag{31}$$

[2] By a greater number of grid points the performance did not improve

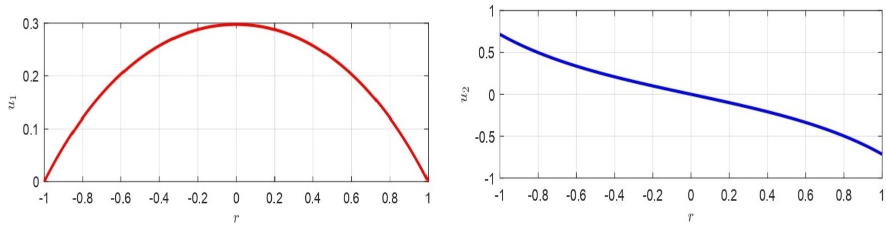

Fig. 2: Recovering of the membrane: $\theta\lambda^2 = 0.5$, $u_1 \leq 2.446$, $u_2 = 0$.

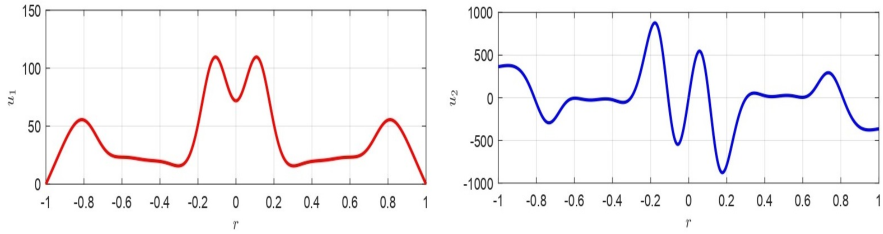

Fig. 3: Recovering of the membrane: $\theta\lambda^2 = 0.5$, $2.447 \leq u_1 \leq 2.453$, $u_2 = 0$.

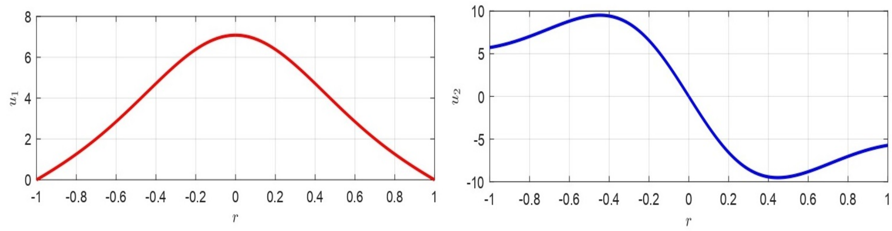

Fig. 4: Recovering of the membrane: $\theta\lambda^2 = 0.5$, $2.454 \leq u_1 \leq 9.474$, $9.63 \leq u_1 \leq 12.7$ and $15.1 \leq u_1 \leq 19.978$, $u_2 = 0$.

from which, being for $\theta\lambda^2 \leq 10^{-6}$ the numerical procedure stably converge, it follows that

$$\theta\lambda^2 > \frac{10^{-18}}{V^2k} \quad \wedge \quad \theta\lambda^2 \geq 10^{-6}$$

from which $V^2k \leq 10^{-12}$. Thus, the range of V^2k ensuring both convergence and stability is $V^2k \in (0, 10^{-12}]$. As already shown, $\forall\theta\lambda^2 \in (0, 10^{-7})$ the procedure does not converge achieving

$$\theta\lambda^2 > \frac{10^{-18}}{V^2k} \quad \wedge \quad \theta\lambda^2 \leq 10^{-7}$$

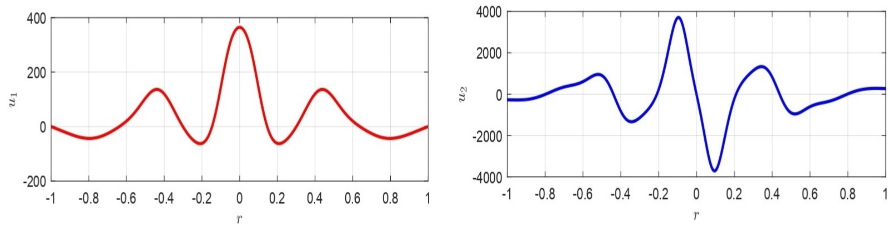

Fig. 5: Recovering of the membrane: $\theta\lambda^2 = 0.5$, $9.475 \leq u_1 \leq 9.62$, $12.71 \leq u_1 \leq 15$ and $u_1 \geq 19.979$, $u_2 = 0$.

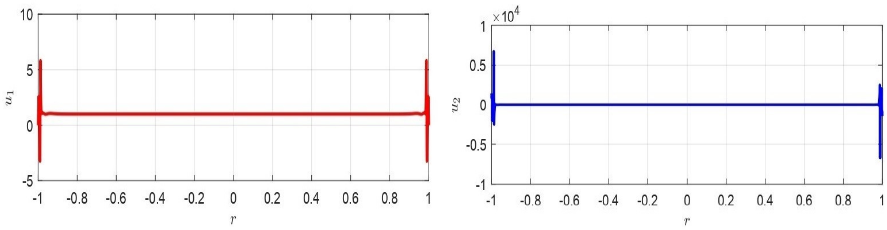

Fig. 6: Recovering of the membrane: $u_1 = 0.1$ and $\theta\lambda^2 = 5 \cdot 10^{-7}$.

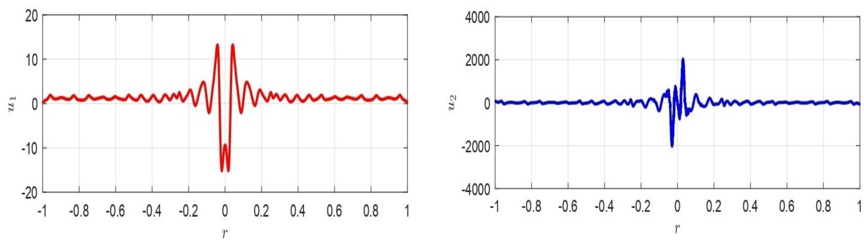

Fig. 7: Recovering of the membrane: $u_1 = 1.2$ and $\theta\lambda^2 = 5 \cdot 10^{-5}$.

so that $V^2k \geq 10^{-11}$. Therefore, $\forall V^2k \in [10^{-11}, +\infty)$ the procedure does not converge. If the procedure converges (also unstably), $\theta\lambda^2 \in [10^{-7}, 10^{-6}]$. Thus,

$$\theta\lambda^2 > \frac{10^{-18}}{V^2k} \quad \wedge \quad 10^{-7} < \theta\lambda^2 < 10^{-6}$$

In this paper, the numerical procedure converges even though, next to the edge, instability phenomena could take place.

No Convergence	Convergence & Instability	Convergence & Stability
$\theta\lambda^2 \leq 10^{-7}$	$10^{-7} < \theta\lambda^2 < 10^{-6}$	$\theta\lambda^2 \geq 10^{-6}$
$V^2k \geq 10^{-11}$	$10^{-12} < V^2k < 10^{-11}$	$V^2k \leq 10^{-12}$
No Ghost Solutions if $\theta\lambda^2 > 10^{-12}$	No Ghost Solutions	No Ghost Solutions

Table 2: Convergence and Stability Areas.

8.1 An Overview on the Ghost Solutions Areas

Starting from (54), setting $r = 0$, the displacement of the membrane at the center of the device, v_0, becomes $v_0 = \frac{k\epsilon_0 V^2}{(1-v(r))^2}$, from which

$$V^2k = \frac{2u_0(1-v(r))^2}{\epsilon_0} \tag{32}$$

that, combining with (31), becomes

$$\theta\lambda^2 > \frac{10^{-18}\epsilon_0}{2\ u_0(1-v(r))^2}. \tag{33}$$

However, $\epsilon_0 \approx 10^{-12}$, $u_0 \approx 10^{-9}$ and $(1-v(r))^2 \approx 10^{-9}$, so that (33) becomes:

$$\theta\lambda^2 > \frac{10^{-18}\epsilon_0}{2v_0(1-v(r))^2} \approx \frac{10^{-18}10^{-12}}{2\ 10^{-9}10^{-9}} \approx 10^{-12}. \tag{34}$$

Thus, $\forall\theta\lambda^2 \in (0, 10^{-12}]$ any solutions could be ghost solutions. Anyway, since $\forall\theta\lambda^2 \in (0, 10^{-7}]$ the numerical method does not converge, it follows that each numerical solution achieved does not represent a ghost solution. Table 2 summarizes the achieved results.

Remark 2 It is worth noting that the presence of ghost solutions are extremely risky for the clinical applications of micropumps. This is due to the fact that a ghost solution is in any case a solution that is not foreseen by the physical-mathematical model. In other words, the numerical procedure detects a deformation of the membrane (and therefore inoculation of the drug) which in reality does not occur.

9 On the Mechanical Properties of the Membrane & the Intended Use of the Micropump

As mentioned above, we can write $\xi|\mathbf{E}|^2 = \frac{\lambda^2}{(1-v(r))^2}$. In addition, taking into account that $\lambda^2 = \frac{\epsilon_0(2R)^2V^2}{2Td^3} = \rho V^2$ with $\rho\frac{\epsilon_0(2R)^2}{2Td^3}$, we can also write

$$\theta|\mathbf{E}|^2 = \frac{\lambda^2}{(1-u(r))^2} = \frac{\epsilon_0(2R)^2V^2}{2Td^3}\frac{1}{1-v(r)^2}.$$

If we then multiply by λ^2 all the above equation, we achieve:

$$\theta\lambda^2 = \frac{\epsilon_0 R^4 V^4}{4T^2 d^6 (1-u(r))^2 |\mathbf{E}|^2}. \tag{35}$$

One can observe that, dimensionless conditions, $d = R = 1$ and $(1-v(r))^2 < 1$. Moreover, $|\mathbf{E}|^2 < \sup |\mathbf{E}|^2$, from which $\frac{1}{|\mathbf{E}|^2} > \frac{1}{\sup |\mathbf{E}|^2}$ so that (35) becomes

$$\theta\lambda^2 = \frac{\epsilon_0 V^4}{4T^2 (1-v(r))^2 |\mathbf{E}|^2} > \frac{\epsilon_0 V^4}{4T^2 (\sup |\mathbf{E}|^2)}. \tag{36}$$

We observe that $\theta\lambda^2$ is a bounded quantity because, if this were not the case, the equation of the model would be reduced to the Laplace equation admitting Newtonian potentials and/or logarithmic potentials as solutions. Then, one can write $\theta\lambda^2 < B$ with B positive constant so that inequality (36) can be written as follows $B > \theta\lambda^2 > \frac{\epsilon_0 V^4}{4T^2(\sup |\mathbf{E}|^2)}$. Then, it is easy to achieve the following inequalities:

$$T > \sqrt{\frac{\epsilon_0 V^4}{4B(\sup |\mathbf{E}|^2)}} \tag{37}$$

or

$$\frac{V^4}{\sup |\mathbf{E}|^2} < \frac{4BT^2}{\epsilon_0}. \tag{38}$$

Then, once the intended use of the micropump has been chosen (for example, for a particular intravenous drug diffuser), the value of external V is fixed, and therefore, through electrostatic calculations, the $\sup |\mathbf{E}|$. Then, once $\frac{V^4}{\sup |\mathbf{E}|^2}$ is known, by means of (37), we obtain the value of T which represents how much tension must be subjected to the membrane in its rest position to deform, under the effect of V, without touching the upper plate. Conversely, once T is selected ((i.e. fixed the value of the mechanical tension when the membrane is in the resting state), we obtain $\frac{V^4}{\sup |\mathbf{E}|^2}$ which satisfies (38). In other words, micro-pumps whose membrane at rest has a mechanical tension T, can be used only in pharmacological diffusion devices whose voltage V (and therefore also $|\mathbf{E}|$) satisfy (38).

Remark 3 It is worth noting that inequality (38) has an important clinical significance. In fact, if the micropump is inserted in an electric device subjected to a given electric voltage V, it is necessary that inside the micropump the material between the two plates produces an electric field whose upper end of its amplitude together with the mechanics of the membrane T satisfy (38). If this does not happen, the drug injection device is malfunctioning and not ensuring the prescribed dosage.

10 Conclusion and Perspectives

Micropumps for drug delivery within the human body represents one of the most important clinical facilities especially with non-cooperative patients (pediatric, oncology patients and so on). Scientific research has produced hospital facilities operating according to the most varied physical principles. Among them, electrostatic micropumps stand out as they are easy to manufacture and require minimal maintenance. The models for such devices describe the behavior of the device in the different operating phases in detail but they are complex and therefore require simplifications for obtaining new and slimmer models that, at least qualitatively, describe the behavior of the device itself. Circular membrane electrostatic micropumps, whose physical-mathematical simplified model is represented by an ordinary nonlinear differential equation of the second order with singularity, are no exception. Furthermore, expressing $|\mathbf{E}|$ as a function of the mean curvature of the membrane opens interesting scenarios regarding the study of the existence, uniqueness and stability of the solution. On the one hand, because the use of mean curvature has provided the possibility of obtaining an algebraic condition that manages the existence of the solution (even if its uniqueness is not assured). Moreover, the use of mean curvature has opened a scenario regarding the connection between the electromechanical properties of the membrane and the intended use of the device. Such peculiarities, although encouraging from a physical-mathematical point of view, should be considered as a first step for future developments where the use of more sophisticated curvature formulations is hoped to highlight in greater detail the link between the material constituting the membrane and the intended use of the device.

Appendix A

A Useful Formulation for MC

Let be B a surface determined rotating a curve M located on the plane orthogonal to xy in a xyz Cartesian system (see Figure 8). It is known that the curve M can be parameterized by a parameter, r, which does not represents the curve-line coordinate [31]. So, a generic point $P(r)$ on M can be defined by

$$P(r) = (a(r), 0, b(r)), \tag{39}$$

with r belonging to $[0, R]$. Moreover, $a(r)$ and $b(r)$ are regular functions such that

$$(a_r(r))^2 + (b_r(r))^2 \geq 0. \tag{40}$$

Finally, M can be parameterized as [31]

$$P(t, r) = (a(r) \cos t, a(r) \sin t, b(r)). \tag{41}$$

We note that $P(r)$ is a natural parameterization ensuring that M is a regular curve. It follows that also S is regular.

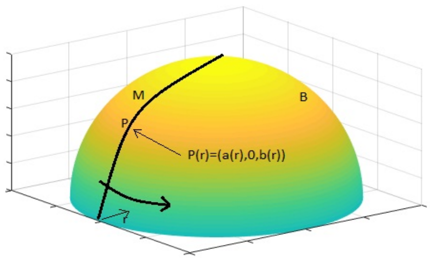

Fig. 8: Curve M located on the surface B on the plane orthogonal to xy in a xyz cartesian system.

Coefficients of First and Second Fundamental Forms
By means of (41), we can write

$$\begin{cases} P_t = (-a(r)\sin t, a(r)\cos t, 0), \\ P_r = (a_r(r)\cos t, a_r(r)\sin t, b_r(r)). \end{cases} \tag{42}$$

Therefore, the coefficients of the first fundamental form, E, F and G become

$$\mathrm{E} = \|P_r(t,r)\|^2 = a^2(r), \quad \mathrm{F} = P_r(t,r)\cdot P_t(t,r) = 0,$$
$$\mathrm{G} = \|P_t(t,r)\|^2 = 1.$$

Being F $= 0$ everywhere, the coordinate lines always result orthogonal each other. From both (42) we can write

$$P_{tt}(t,r) = (-a(r)\cos t, -a(r)\sin t, 0), \tag{43}$$

$$P_{tr}(t,r) = (-a_r'(r)\sin t, a_r(r)\cos t, 0), \tag{44}$$

$$P_{rr}(t,r) = (a_{rr}(r)\cos t, a_{rr}(r)\sin t, b_{rr}(r)). \tag{45}$$

We observe that

$$P_t(t,r)\times P_r(t,r) = a(r)(b_r(r)\cos t, b_r(r)\sin t, -a_r(r)) \tag{46}$$

and the unit normal vector $\underline{\hat{\mathbf{n}}}$ to M in $P(t,r)$ becomes

$$\frac{\Big(P_t(t,r)\times P_r(t,r)\Big)}{\|P_t(t,r)\times P_r(t,r)\|} = (b_r(r)\cos t, b_r(r)\sin t, -a_r(r)).$$

Hence, the coefficients of the second fundamental form, e, f and g become

$$\mathrm{e} = P_{rr}(t,r)\cdot\underline{\hat{\mathbf{n}}} = -a(r)b_r(r), \tag{47}$$
$$\mathrm{f} = P_{rt}(t,r)\cdot\underline{\hat{\mathbf{n}}} = 0,$$
$$\mathrm{g} = P_{tt}(t,r) = a_{rr}(r)g_r(r) - a_r(r)b_{rr}(r).$$

Computation of the Mean Curvature $MC(t,r)$
The principal curvatures, $\overline{pc}_1(t,r)$ and $\overline{pc}_2(t,r)$, can be computed solving the equation $(\mathrm{e} - k\mathrm{E})(\mathrm{g} - pc\mathrm{G}) - (\mathrm{f} - pc\mathrm{F})^2 = 0$ achieving

$$\overline{pc}_1(t,r) = -\frac{b_r(r)}{a(r)} \tag{48}$$

and

$$\overline{pc}_2(t,r) = a_r(r)b_r(r) - a_r(r)b_{rr}(r). \tag{49}$$

$MC(t,r)$, known both $\overline{pc}_1(t,r)$ and $\overline{pc}_2(t,r)$, is computed as follows [31]

$$MC(t,r) = \frac{1}{2}(\overline{pc}_1(t,r) + \overline{pc}_2(t,r)), \tag{50}$$

obtaining

$$MC(t,r) = \frac{1}{2}\Big(- \frac{b_r(r)}{a(r)} + a_r(r)b_r(r) - a_r(r)b_{rr}(r)\Big). \tag{51}$$

It is worth nothing that M is located on the plane $y = 0$. Then, $a(r) = r$ and $b(r) = v(r)$, so that $a_r(r) = 1$ and $a_{rr}(r) = 0$, although by $b(r) = v(r)$ we achieve $b_r(r) = v_r(r)$ and $b_{rr} = v_{rr}(r)$. We observe that both $a_r(r)$ and $b_r(r)$ satisfy (40). Finally, we can write $MC(r) = -\frac{1}{2}\Big(\frac{v_r(r)}{r} + v_{rr}(r)\Big)$.

Appendix B

Proof of Proposition 1
Exploiting (11), let us set $v_1(r)$ and $v_2(r)$ as $v_1(r) = 0 \ \ \forall r \in [0,R]$ and

$$v_2(r) = \overline{v}(r) = \frac{k\epsilon_0 V^2}{2d^*}\Big(1 - \Big(\frac{r}{R}\Big)^2\Big)$$

(see Figure **??**). It is simply to verify that, by construction, $v_1(r) < v_2(r)$ and both $v_1(r)$ and $v_2(r)$ are clearly twice continuously differentiable functions. Then, from both (19) and (20), we can write:

$$\begin{aligned} v_{1rr}(r) + F(r, v_1(r), v_{1r}(r)) = \\ = v_{1rr}(r) + \frac{v_{1r}(r)}{r} + \frac{(1 - v_1(r) - d^*)^2}{\theta\lambda^2} > 0, \end{aligned} \tag{52}$$

$$\begin{aligned} v_{2rr}(r) + F(r, v_2(r), v_{2r}(r)) = \\ = u_{2rr}(r) + \frac{v_{2r}(r)}{r} + \frac{(1 - v_2(r) - d^*)^2}{\theta\lambda^2} < 0. \end{aligned} \tag{53}$$

We note that, when $u_1(r) = 0 \ \forall r \in [0, R]$, we have $v_{1r}(r) = 0$. Then, if $\theta\lambda^2 > 0$, (52) is verified. Moreover, knowing that

$$v_2(r) = \frac{k\epsilon_0 V^2}{2d^{*2}}\Big(1 - \Big(\frac{r}{R}\Big)^2\Big), \tag{54}$$

we can write $v_{2r}(r) = -\frac{\epsilon_0 k V^2}{d^{*2}}\frac{r}{R^2}$ and $v_{2rr}(r) = -\frac{\epsilon_0 k V^2}{d^{*2}R^2}$. Then, the inequality (53) becomes

$$\frac{\epsilon_0 k V^2}{\theta\lambda^2}\Big(1 - \frac{1}{2d^{*2}}\Big(1 - \Big(\frac{r}{R}\Big)^2\Big)^2 < \frac{\epsilon_0 k V^2}{R^2 d^{*2}} \tag{55}$$

It is easy to note that, in (55),

$$\frac{\epsilon_0 k V^2}{\theta\lambda^2}\Big(1 - \frac{1}{2d^{*2}}\Big(1 - \Big(\frac{r}{R}\Big)^2\Big)^2 < 1$$

so that if we impose $\frac{1}{\theta\lambda^2} < \frac{2\epsilon_0 k V^2}{R^2 d^{*2}}$, it follows that $\theta\lambda^2 > \frac{R^2 d^{*2}}{2\epsilon_0 k V^2}$. In addition, according to Result 1, we must prove that $P(r, v(R), v'(r)) = \frac{v_r(r)}{r} + \frac{(1-v(R))^2}{\theta\lambda^2}$ satisfies the condition (18). Then, we can write:

$$\begin{aligned} F(r, v(r) - u(r), v_r(r)u_r(r)) &= \\ = \frac{v_r(r)}{r} + \frac{(1-v(r))^2}{\theta\lambda^2} &= -\frac{v_r(r)}{r} - \frac{(1-v(r))^2}{\theta\lambda^2} = \\ = \frac{(v_r(r) - u_r(r))}{r} + \frac{\{(1 - v(r) - 1 + u(r))(1 - v(r) + 1 - u(r))\}}{\theta\lambda^2} &= \\ = \frac{(v_r(r) - u_r(r))}{r} - (v(r) - u(r))\frac{(2 - (v(r) + u(r)))}{\theta\lambda^2} &\geq \\ = \frac{(v_r(r) - u_r(r))}{r} - \frac{2(v(r) - u(r))}{\theta\lambda^2} &= \\ = N_2(r)(v_r(r) - u_r(r)) + M_1(r)(v(r) - u(r)). \end{aligned} \tag{56}$$

Moreover, we observe that the following chain of inequalities holds:

$$\begin{aligned} \frac{v_r(r) - u_r(r)}{r}\frac{(v(r) - u(r))(2 - (v(r) + u(r))}{\theta\lambda^2} &\leq \\ \leq \frac{v_r(r) - u_r(r)}{r} - \frac{A(v(r) - u(r))}{\theta\lambda^2} &= \\ = N_1(r)(v_r(r) - u_r(r)) + AM_2(r)((v(r) - u(r))). \end{aligned} \tag{57}$$

We observe that in (57) the quantity $2-(v(r)+u(r))$ is greater than or equal to zero. Then, there exists a constant A such that $2-(v(r)+u(r)) > A > 0$ holds. Finally, we observe that Result 1 requires that $v_{1r}(m) \geq v_{2r}(m)$. In fact, since $a = r = 0$, we achieve $v_{1r}(m) = v_{1r}(0) = 0$. And again, $v_{2r}(m) = v_{2r}(0) = 0$. In addition, we observe that $v_1(R) = v_2(R) = 0$ concluding the proof of the theorem.

Appendix C

Proof of Proposition 2
From the chain of inequality (57), we can write

$$N_1(r)v_r(r) + M_2(r)Av(r) = \frac{v_r(r)}{r} - \frac{Av(r)}{\theta\lambda^2}.$$

Then, using Result 2, we write the following Bessel differential equation

$$v_{rr}(r) + \frac{v_r(r)}{r} - \frac{Av(r)}{\theta\lambda^2} = 0. \tag{58}$$

The general solution for (58) can be written as a linear combination of two linearly independent Bessel functions of the first and second kind of zeroth order, $J_0(\sqrt{(\theta\lambda^2)^{-1}A}r)$ and $Y_0(\sqrt{(\theta\lambda^2)^{-1}A}r)$. Specifically, with B_1 and B_2 constant, we can write [33]:

$$\begin{aligned} v(r) &= B_1 J_0\Big(\sqrt{(\theta\lambda^2)^{-1}A}r\Big) + B_2 Y_0\Big(\sqrt{(\theta\lambda^2)^{-1}A}r\Big) = \\ &= B_1 + B_1(2^{2s}(s!)^2)^{-2}\sum_{s=1}^{\infty}(-1)^s\Big(\sqrt{(\theta\lambda^2)^{-1}A}r\Big)^{2s} + \\ &\quad +2(\lambda)^{-1}B_2\Big(\overline{b} + \ln\Big(0.5\Big(\sqrt{(\theta\lambda^2)^{-1}A}r\Big)\Big)\Big) \\ &\quad \Big[1 + \sum_{s=1}^{+\infty}(2^s(s!))^{-2}(-1)^2(\sqrt{(\theta\lambda^2)^{-1}A}r)^{2s} + \\ &\quad + \sum_{s=1}^{\infty}(2^{2s}(s!)^2)^{-2}(-1)^{s+1}\overline{H}_s\Big(\sqrt{(\theta\lambda^2)^{-1}A}r\Big)^{2s}\Big], \end{aligned} \tag{59}$$

where $\overline{b} = 0.5772$ represents the Euler-Mascheroni constant and $\overline{H}_s$ is computed as $1 + 2^{-1} + 3^{-1} + \cdots + s^{-1}$.
It is worth nothing that, the more r approaches zero, the more J_0 approaches 1. In addition, being $Y_0 = \ln\Big(0.5\sqrt{(\theta\lambda^2)^{-1}A}r\Big)$, Y_0 has a logarithmic singularity when r is equal to zero. However, with $B_1 \neq 0$ and $B_2 = 0$ the general solution can be written as follows:

$$v(r) = B_1\left[1 + \sum_{s=1}^{+\infty}(2^{2s}(s!)^2)^{-2}(-1)^s\Big(\sqrt{(\theta\lambda^2)^{-1}A}r\Big)^{2s}\right].$$

Then, we have found a solution for the equation (58) (different from $v(r) = 0$). As a consequence, the uniqueness of the solution for the problem under study is not ensured. This remarks concludes the proof of the Theorem.

References

1. Mahnama et al., A survey on the applications of implantable micropump systems in drug delivery, 11. 123–131page numbers. Bentham Science Publishers, Boca Raton London New York Washington, D.C. (2014)
2. H.J. Lee and N. Choi and E.S. Yoon and P. Kunal, MEMS devices for drug delivery, Advanced Drug Delivery Reviews, 128, 132–147 (2018)
3. C. Joshita and S. Sreeja and S. Radha, A review on micropumps for drug delivery system, IEEE International Conference on Wireless Communications, Signal Processing and Networking (WiSPNET 2017), 186–190 (2017)
4. M.J. Rathbone and B.K. Drummond and I.H. Tucker, The oral cavity as a site for systemic drug delivery, Advanced drug delivery reviews, 12, 1–22 (1994)
5. D.D. Breimer, Future challenges for drug delivery research, Advanced drug delivery reviews, 33, 265–268 (1998)
6. F.R. Munas and A.Y.W. Ranjith and P. Kunal, Review on MEMS based micropumps for biomedical applications, Int. J. Innov. Res. Sci. Eng. Technol, 4, 5602–5615 (2015)
7. N. Rajgor and M. Patel amd V.H. Bhaskar, Implantable Drug Delivery Systems: An Overview, Surgical Neurology International, 2(2), 122–131 (2011)
8. R. Fernandes and D.H. Gracias, Self-folding polymeric containers for encapsulation and delivery of drugs, Advanced drug delivery reviews, 64, 4, 1579–1579 (2012)
9. K. Yeu-Chun and Y.H. Park and M.R. Prausnitz, Microneedles for drug and vaccine delivery, 64(14), 1589–1568 (2012)
10. H.J. Lee amnd Y. Son and K. Jeongyeon and C. Lee and E.S. Yoon and I.J. Cho, A multichannel neural probe with embedded microfluidic channels for simultaneous in vivo neural recording and drug delivery, 15(6), 1590–1597 (2015)
11. F. Munoz and A. Gursel and W. Li, A review of drug delivery systems for capsule endoscopy, Advanced drug delivery reviews, 71, 77–85 (2014)
12. M.N. Yasin and D. Svirskis and A. Seyfoddin and D. Ilva, Implants for drug delivery to the posterior segment of the eye: A focus on stimuli-responsive and tunable release systems, Journal of Controlled Release, 196, 208–2011 (2014)
13. P. Suprio and N. Suraj and A. Arfat and P. Kunal, MEMS-based controlled drug delivery systems: a short review, Polymer-Plastics Technology and Engineering, 55(9), 965–975 (2016)
14. M. Cacciola and S. Calcagno and G. Megali and F.C. Morabito and D. Pellicanó and M. Versaci, FEA design and misfit minimization for in-depth flaw characterization in metallic plates with Eddy current nondestructive testing, IEEE Transactions on Magnetics, 45(3), 1506–1509 (2009)
15. M.N. Postorino and M. Versaci, A neuro-fuzzy approach to simulate the user mode choice behaviour in a travel decision framework, International Journal of Modelling and Simulation, 28(1), 64–71 (2008)
16. W.L. Bernard and H. Kahn and H. Heuer and M.A. Huff, A titanium-nickel shape-memory alloy actuated micropump, 196, 208–221 (1997)
17. W.L. Bernard and H. Kahn and H. Heuer and M.A. Huff, Thin-film shape-memory alloy actuated micropumps, Journal of Microelectromechanical systems, 7(2), 245–251 (1998)
18. M.T. Saif and B.E. Alaca and H. Sehitoglu, Analytical modeling of electrostatic membrane actuator for micro pumps, Journal of Microelectromechanical systems, 8(3), 335–345 (1999)
19. H. Liu, Implicit Runge-Kutta methods based on Lobatto quadrature formula, International Journal of Computer Mathematics, 82(1), 77–88 (2005)
20. H.O. Al-Humedi and A. Al-Saadaqwi, Spectral shifted Jacobi-Gauss-Lobatto methodology for solving two-dimensional time-space fractiona bioheat mode,m AIP Conference Proceedings, 2235, 020011 (2020)
21. P. Di Barba and L. Fattorusso and M. Versaci, Electrostatic Field in Terms of Geometric Curvature in Membrane MEMS Devices, Communications in Applied and Industrial Mathematics, 8(1), 165–184 (2017)
22. J.A. Pelesko and D.H.Bernestein, Modeling MEMS and NEMS, Chapman & Hall/CRC Press, Boca Raton London New York Washington, D.C. (2003)

23. D. Cassani and M. d'O and N. Ghoussoub, On a Fourth Order Elliptic Problem with a Singular Nonlinearity, Nonlinear Studies, 9, 189–209 (2009)
24. M Versaci and F.C. Morabito, Membrane Micro Electro-Mechanical Systems for Industrial Applications, Handbook of Research on Advanced Mechatronic Systems and Intelligent Robotics, IGI Global (2019)
25. M. Versaci and A. Jannelli and G. Angiulli, Electrostatic Micro-Electro-Mechanical-Systems (MEMS) Devices: A Comparison among Numerical Techniques for Recovering the Membrane Profile, IEEE ACCESS, 8, 125874–125886 (2020)
26. M. Versaci and G. Angiulli and L. Fattorusso and A. Jannelli, On the Uniqueness of the Solution for a Semi-Linear Elliptic Boundary Value Problem of the Membrane MEMS Device for Reconstructing the Membrane Profile in Absence of Ghost Solutions, International Journal of Non-Linear Mechanics, 109, 24–31 (2019)
27. P. Di Barba and L. Fattorusso and M. Versaci, A $2D$ Non-Linear Second-Order Differential Model for Electrostatic Circular Membrane MEMS Devices: A Result fo Existence and Uniqueness, Mathematics, MDPI, 7(1193), 1–18 (2019)
28. G. Angiulli and A. Jannelli and F.C. Morabito and M. Versaci, Reconstructing the Membrane Detection of a 1D Electrostatic-Driven MEMS Device by the Shooting Method: Convergence Analysis and Ghost Solutions Identiffication, Computational and Applied Mathematics, 37(4), 4484–4498 (2018)
29. M. Versaci and P. Di Barba and F.C. Morabito, Curvature-dependent electrostatic field as a principle for modelling membrane-based mems devices. A review, Membranes MDPI, 10(11), 1-51 (2020)
30. S.P. Timoshenko and S. Woinowsky-Krieger, Theory of plates and shells, McGraw-hill (1959)
31. L.W. Tu, Differential geometry: connections, curvature, and characteristic classes, Springer (2017)
32. P.B. Bailey et al., Nonlinear Two Point Boundary Value Problems, Academic Press (1968)
33. F. Bwmann, Introduction o Bessel Functions, Courier Corporation (2012)